frontiers | Frontiers in Soft Matter

TYPE Original Research
PUBLISHED 06 December 2023
DOI 10.3389/frsfm.2023.1306346

OPEN ACCESS

EDITED BY
Nimita Jebaranjitham J.,
Women's Christian College, India

REVIEWED BY
Venkatesh Srinivasan,
University of Maryland, United States
V. Lincy,
National Taiwan University of Science and Technology, Taiwan

*CORRESPONDENCE
Jayati Sarkar,
jayati@chemical.iitd.ac.in

RECEIVED 03 October 2023
ACCEPTED 21 November 2023
PUBLISHED 06 December 2023

CITATION
Agarwal S, Lu M and Sarkar J (2023), Fabrication of micropatterned thin films through controlled phase separation of polystyrene/polydimethylsiloxane blends by spin coating.
Front. Soft Matter 3:1306346.
doi: 10.3389/frsfm.2023.1306346

Fabrication of micropatterned thin films through controlled phase separation of polystyrene/polydimethylsiloxane blends by spin coating

Swarnima Agarwal[1,2], Mingyuan Lu[2] and Jayati Sarkar[1]*

[1]Department of Chemical Engineering, Indian Institute of Technology Delhi, New Delhi, India, [2]School of Mechanical and Mining Engineering, Faculty of Engineering, Architecture and Information Technology, The University of Queensland, Brisbane, QLD, Australia

In this study, we blended two readily available polymers, polydimethylsiloxane (PDMS), a semi-crystalline polymer, and polystyrene (PS), an amorphous polymer, both having widely varying physical properties. The blend is then spin coated to form a thin film. We investigated the effects of relative polymer concentration, spin coating speed, and environmental factors, such as temperature, on the ultimate morphologies of the phase-separated thin films. It was found that it is possible to regulate the morphologies of the thin films to achieve desirable microstructures such as spherical droplets, holes, bi-continuous lamellar structures, and tubules by controlling the fabrication conditions. The polymer blend films with higher PS concentrations were shown to form a bilayer system with an upper PS-rich layer due to the thermodynamic instability of the film caused by the rapid evaporation of solvent, while films with higher PDMS concentrations exhibited cohesive forces that engendered microtubule formation and led to high surface roughness.

KEYWORDS

polystyrene/polydimethylsiloxane blends, phase separation, micropatterns, thin films, spin coating

1 Introduction

Polymer thin films enjoy a wide application across various fields of research, such as electronics, optics, and biotechnology (Xia et al., 1996; Sirringhaus, Tessler, and Friend, 1998; Jager, Smela, and Inganäs, 2000). The diverse range of applications requires films with a wide array of surface morphologies, including uniform and smooth surfaces and specially ordered patterns of varying length scales. One cost-effective approach to creating patterned surfaces involves exploiting the inherent surface instability of thin polymer films, including phenomena like dewetting (Sharma and Reiter, 1996; Xue and Han, 2011) and phase separation (Budkowski, 1999), both of which fall under the category of "bottom-up" methods. In the context of thin films, phase separation often coincides with dewetting (Müller-Buschbaum et al., 2005). Dewetting occurs when an unstable or metastable thin polymer film on a non-wetting solid surface gains sufficient mobility due to thermal or solvent vapor annealing. The typical dewetting process involves the formation and growth of holes, the merging of these holes to create ribbons, and the eventual disintegration of ribbons into droplets (Kargupta and Sharma, 2001; Müller-Buschbaum, 2003). Controlled dewetting offers a convenient and effective means

of generating ordered structures on a micro/nano-meter scale, which can be tailored to mimic natural structures to achieve properties required for certain niche applications (Xue, Zhang, and Han, 2012). For instance, they can be used to create self-cleaning and water-repellent coatings based on lotus leaf structure (Latthe et al., 2014), antireflective optical coatings that imitate a moth's eye (McDougal et al., 2019), and photonics and optoelectronics films that resemble the surface of butterfly wings (McDougal et al., 2019). Polydimethylsiloxane (PDMS) has good optical transparency in the visible and near-infrared spectra. Blending with polystyrene (PS) can modify the refractive index, making it useful for optical devices such as lenses, waveguides, or micro-opto-electromechanical systems (MOEMSs) (Köse et al., 2005; R; Luo et al., 2020). They can also be used for anti-fouling coatings in marine applications that replicate the surface of 'shark' skin (Fu et al., 2017). PDMS is known for its low surface energy, which helps in resisting the adhesion of biofouling organisms. Blending PDMS with PS can enhance the coating's mechanical strength while maintaining its anti-fouling properties, making it useful for marine applications or medical devices prone to biofouling (Mo et al., 2021). The biocompatible nature of PDMS makes it suitable for applications in biomedical devices. Blending with PS can make the material more robust for various medical applications, such as implantable devices or controlled drug release systems (T. Luo et al., 2023; Arias-Zapata et al., 2016). Patterned PDMS films formed due to isotropic contact instability show a significant influence on selective oil adsorption from oil–water mixtures, making them useful as separation and oil-recovery membranes (Basu and Sarkar, 2019).

Spin coating is a widely used deposition technique for polymer thin films, leveraging phase separation and dewetting phenomena to achieve diverse surface morphologies (Walheim, Ramstein, and Steiner, 1999; Ton-That et al., 2000; Raczkowska et al., 2004; Escalé et al., 2012). However, it is important to note that the resultant structures produced through spin coating are often not in a state of equilibrium due to rapid solvent evaporation, slow phase separation, and dewetting kinetics (Basu et al., 2021). To attain equilibrium, annealing of the thin film is required to facilitate the arrested nanostructures to achieve stability (Ton-That et al., 2000). Some of the various parameters that have been studied to understand their effect on the resulting film structures are film thickness (Tanaka et al., 1996), solvent (Arias et al., 2002; Cui et al., 2006), molecular weight (Li, 2003), substrate (Boltau et al., 1998; Björström et al., 2007; Wei et al., 2009), and formulation of polymer blends (El-Mabrouk et al., 2007; Zuyderhoff et al., 2008; Sohn et al., 2011).

Indeed, surface-induced morphological phase separation in an immiscible polymer blend thin film spin cast from a common solvent has long been explored and has garnered considerable attention due to its potential applications in areas such as dielectric coatings, the modulation of optical and wetting characteristics of surfaces, and gaining insights into how confinement affects phase separation (Tu, et al., 2019a; Tu, et al., 2019; Bhandaru, 2020; Dhara and Mukherjee, 2021; Saleem et al., 2023). Polystyrene and poly(metha methacrylate) (PMMA) immiscible blends are among the systems that have been studied most extensively (Das et al., 2020; Guo and Ren, 2021; Mrđenović et al., 2022; Cai et al., 2023). Walheim et al. (1997) utilized a selective dissolution approach to fabricate PS/PMMA film with phase-separated domain structures. Tanaka, Takahara, and Kajiyama (1996) produced phase-separated structures in PS/PMMA films using the spin-coating method. The formation of these surface structures was attributed to either frozen chain conformation or aggregation, preventing the formation of a PS-rich overlayer due to rapid solvent evaporation. Ton-That, Shard, and Bradley (2002) explored the relationship between the PMMA concentration and the size of the structures in the film. They observed that the size of the structures increased with the increasing solution volume and PMMA concentration. The size increase is due to the incomplete dewetting of PMMA from the underlying PS, with structure size increasing linearly with film thickness square for a given PMMA/PS ratio. Some of the studies exploring the formation of composite films are summarized in Table 1.

Despite the occurrence of phase separation, blending two amorphous polymers often does not lead to the formation of micropatterned structures in thin films. However, introducing a crystalline polymer into the blend can result in the formation of unique structures during spin coating, driven by the interplay between phase separation, dewetting, and crystallization. For example, Zhao and Ding (2010) demonstrated the formation of vertically stratified structures by crystallization and lateral phase separation in a crystalline poly(3-hexylthiophene) (P3HT)/poly (ethylene glycol)s (PEG) system. Several studies have reported that phase separation in ultrathin PMMA/polyethylene oxide (PEO) films significantly impacts the crystallization process and crystal shape, resulting in distinctions from those observed in pure PEO films (Okerberg, Marand, and Douglas, 2008; M; Wang, Braun, and Meyer, 2004; Ferreiro et al., 2002; M; Wang, Braun, and Meyer, 2003).

In this study, we demonstrated the ability to create unique surface structures through phase separation and dewetting in thin films formed by blending amorphous PS with semi-crystalline PDMS. Blending PS, an amorphous polymer, with PDMS, a semi-crystalline polymer, for spin-coated thin films can offer a unique set of benefits due to the combination of properties from both polymers. Amorphous polymers like PS typically have good transparency and mechanical strength, while semi-crystalline polymers like PDMS offer flexibility and elasticity. Blending them can result in thin films with a balanced combination of transparency, strength, and flexibility. The amorphous nature of PS can make it brittle, but blending it with a semi-crystalline polymer like PDMS can enhance toughness and ductility. This combination is particularly useful in applications where mechanical durability is essential. Amorphous polymers tend to have lower melting points than semi-crystalline polymers. Blending PS and PDMS can allow for the adjustment of the thermal properties of the thin film, making it suitable for a broader range of temperature conditions. Blending a semi-crystalline polymer with an amorphous polymer can sometimes improve the processability of the blend. This is crucial for spin coating, as it ensures that the thin film can be uniformly deposited on the substrate. The combination of amorphous and semi-crystalline characteristics expands the range of potential applications. For example, such blended films may find use in flexible electronics, sensors, or other applications where a combination of transparency, mechanical strength, and flexibility

TABLE 1 Summary of studies associated with micropatterned thin films.

S. no.	Polymer	Thin-film fabrication method	Significant outcome	Reference
1	Poly(3,4-ethylenedioxythiophene):poly(styrenesulfonate) (PEDOT:PSS) and polydimethylsiloxane (PDMS)	Spreading	Use of a surfactant, Triton X-100, enhances PEDOT: PSS-PDMS films, enabling stretchable conductors for electronics	Luo et al. (2020)
2	Polystyrene (PS)/polyisoprene (PI)	Spin coating	Substrate chemistry shapes polymer blend film topography, enabling lithographic templates	Budkowski et al. (2003)
3	Polystyrene/poly(methyl methacrylate) (PS/PMMA)-AuNP	Spin coating	Addition of AuNPs enable one-step spin coating for thin polymer bilayer formation	Das et al. (2020)
4	Polyvinyl pyrrolidone (PVP)/polyvinyl alcohol (PVA)	Dip coating	Optimized PVA/PVP blend enhances CO_2 permeance for efficient gas separation	Helberg et al. (2020)
5	Poly(3-hexylthiophene-2,5-diyl) (P3HT) and poly(methyl methacrylate) (PMMA)	Spin coating	Efficient one-step spin coating enhances NO_2 sensitivity in high-performance gas sensors	Hou et al. (2019)
6	ZnO over chitosan/polyvinylpyrrolidone (CHP) substrate	Solvent and drop casting	Biodegradable CHP substrate with ZnO film enables flexible and efficient H_2 sensing	Kumar et al. (2020)

is desirable. PDMS is known for its excellent adhesion properties and hydrophobic nature. Blending it with PS can enhance the overall adhesion of the thin film while allowing for control over wetting properties, which is crucial in applications such as microfluidics. Both PS and PDMS are generally compatible with spin coating, making the blending process suitable for thin-film deposition techniques commonly used in microfabrication and other industries (Kästner et al., 2013; Ye et al., 2013).

To our knowledge, blending an amorphous polymer with a semi-crystalline polymer to produce unique patterned films has never been explored. The current study demonstrates that a multitude of morphological patterns can be created by the spin coating of a blended PS–PDMS solution. Spin coating is a relatively simple, cheap technique that is widely used as a precursor step for lithography for the creation of patterned films. It was demonstrated that controllable formation of desirable morphologies in the resulting thin films can be achieved via spin coating of the PS/PDMS blended solution followed by phase separation. This is a highly significant observation, as it has the potential to reduce our dependency on the highly complicated process of lithography to create patterned thin films for use in various applications such as optics, electronics, and biomedical coatings.

The morphology of phase-separated structures in polymer thin films was examined, and the effects of the polymer blend concentrations, spin-coating temperature, and speed on the film morphologies were also studied.

2 Materials and methods

2.1 Materials

PS pellets used in the experiment were supplied by CDH Fine Chemicals Pvt. Ltd. (New Delhi, India) and were used without any additional processing. PDMS was purchased from Dow Chemical Company (United States) as a two-part silicone elastomer kit consisting of a silicone elastomer and a cross-linking agent under the trade name SYLGARD™ 184. PDMS was prepared by mixing the elastomer with the crosslinker in a ratio of 10:1, the mixture was degassed until a clear, and a viscous liquid was obtained. Toluene, a common solvent, was sourced from Thermo Fisher Scientific and used as received.

2.2 Fabrication of PS/PDMS blended thin films

Figure 1 shows a schematic of the film fabrication process. To prepare PS solutions, the PS pellets were dissolved in toluene to obtain solutions of 1%, 2%, and 5% weight by volume while stirring with a magnetic stirrer at 1000 rpm. The PS/PDMS blended solutions were prepared by adding PDMS to the PS solution to obtain PS/PDMS ratios of 1:1, 2:1, 5:1, and 1:5. The blended solutions were then stirred with a magnetic stirrer at 1000 rpm for 2 h to ensure thorough mixing of the two polymers. The glass substrates for spin coating were cleaned by sonication in acetone and then DI water for 15 min each, followed by drying with a stream of N_2. This was carried out to ensure that the surface of the substrate was free of any dust and contaminants. The cleaned glass substrates were then spin coated with the blended solutions using a spinNXG-P1 system at 1,000, 3,000, 5,000, and 8,000 rpm for 30 s to produce PS/PDMS thin films.

The same process was then repeated at 70°C to deposit another set of films. A deposition temperature of 70°C was chosen for spin coating, keeping in mind the glass transition temperature of PS (100°C), the optimum curing temperature of PDMS (60°C–80°C), and the boiling point of toluene (110°C), which was used as the common solvent for polymer blending and spin coating. An optimum temperature of 70°C is recommended to avoid the issues associated with solvent evaporation, which could lead to a change in solution concentration. It also ensures that PDMS is still in an uncured form in the solution.

Both sets of films were then kept at 120°C under a vacuum of 500 mm Hg pressure in an oven for 24 h to facilitate solvent evaporation and stabilize the phase separation pattern.

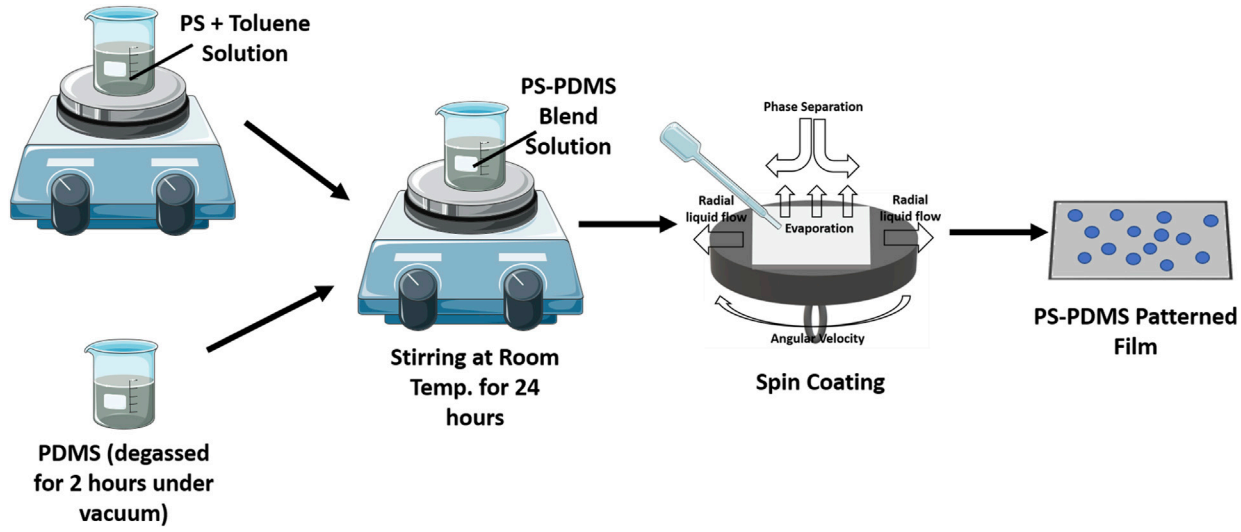

FIGURE 1
Schematic diagram of PS/PDMS blend film formation via spin coating.

2.3 Characterization of the thin films

The morphology of the blended thin films was observed using an optical microscope (OM) in a reflected mode (DCM-295, Leica Microsystems, Germany). Fluorescence microscopy (UTVIX-2, Olympus Corporation, Japan) was used to differentiate the PS and PDMS phases in the film. Rhodamine B dye was used to stain PDMS and was spin coated on the top of the blended film for 30 s at 1000 RPM. This hydrophobic dye naturally emits red fluorescence and can penetrate PDMS while remaining impenetrable in PS (Virumbrales-Muñoz et al., 2019). The OM images were processed using ImageJ software to measure the size of the microstructures present in the thin films.

The height and roughness of the thin films were assessed by atomic force microscopy (AFM) (MFP3D-BIO, Asylum Research, Oxford Instruments, United States) and analyzed through open-source software Gwyddion. The SEM morphology of the thin films was observed using a ZEISS EVO 18 microscope.

3 Results

Figure 2 illustrates the variation in size and morphology of patterned structures formed by the phase separation in PS and PDMS thin films as the blend concentration and spin-coating speed are varied. The columns (i–iv) of each row in Figure 2 display results for coating speeds of 1,000, 3,000, 5,000, and 8,000 RPM, respectively. Figure 2A displays the phase separation pattern of 1:1 (PS/PDMS) blends. Figure 2A shows the appearance of a bilayer structure with two phases, each formed of a separate polymer layer. The darker, discontinuous regions visible in the images show the exposed background layer because of the dewetting of the top polymer layer. The structures of the dewetted holes appear to be polygonal, amorphous, and coarsened. When the blend concentration is 2:1 (PS/PDMS), the morphology consists of more circular dewetted structures in the film, as shown in Figure 2B. The morphology of the blended thin films when the concentration is 5:1 (PS/PDMS) is shown in Figure 2C. These films have perfect circular structures; however, the density of the dewetted structures is significantly lower. A higher polymer concentration of PS is observed to suppress dewetting to a large extent. An increase in spin-coating speed or centrifugal force is found to engender a smaller dewetted circle size and a greater density, as evident from the Figs. i–iv in each of the rows of Figures 2A–C.

Figure 2D (i–iv) show the morphology of the film when the PDMS concentration is 1:5 (PS/PDMS). The structures formed when the PDMS concentration is higher than PS concentration are different from those seen in the previous row of figures. The elevated regions, as depicted by the white regions in the optical microscope under the reflection mode, show spherical agglomeration. However, as the spin-coating speed increases, two opposing phenomena are observed. From Figure 2D (i–ii), it can be seen that higher shear caused by higher centrifugal force helps decrease the sphere size. However, higher centrifugal force (at 5,000 rpm) also helps the sphere to come closer and either coarsen as observed in Figure 2D (iii) or form an elongated tubular structure because of coarsening and excessive stretching (Figure 2D (iv) (at 8,000 rpm)). The tubules are seen to arrange in a radially outward direction because of the underlying high spin-coating rate. The elevated rims of the dewetting polymer, the polygonal dewetted region of the underlying polymer of Figure 2A (iv), the circular dewetted regions of Figure 2B (iv) and Figure 2C (iv), and the elevated tube-like structures of Figure 2D (iv) can be verified from the SEM images of these structures provided in Supplementary Figure S1.

Figures 3A–D show, respectively, the fluorescence images of Rhodamine B-exposed blended films spin coated at 8,000 rpm and having PS/PDMS ratios of 1:1, 2:1, 5:1, and 1:5, respectively. Figures 4A–D show the elemental mapping via line EDX of the blended films spin coated at 8000 rpm and having PS/PDMS ratios of 1:1, 2:1, 5:1,

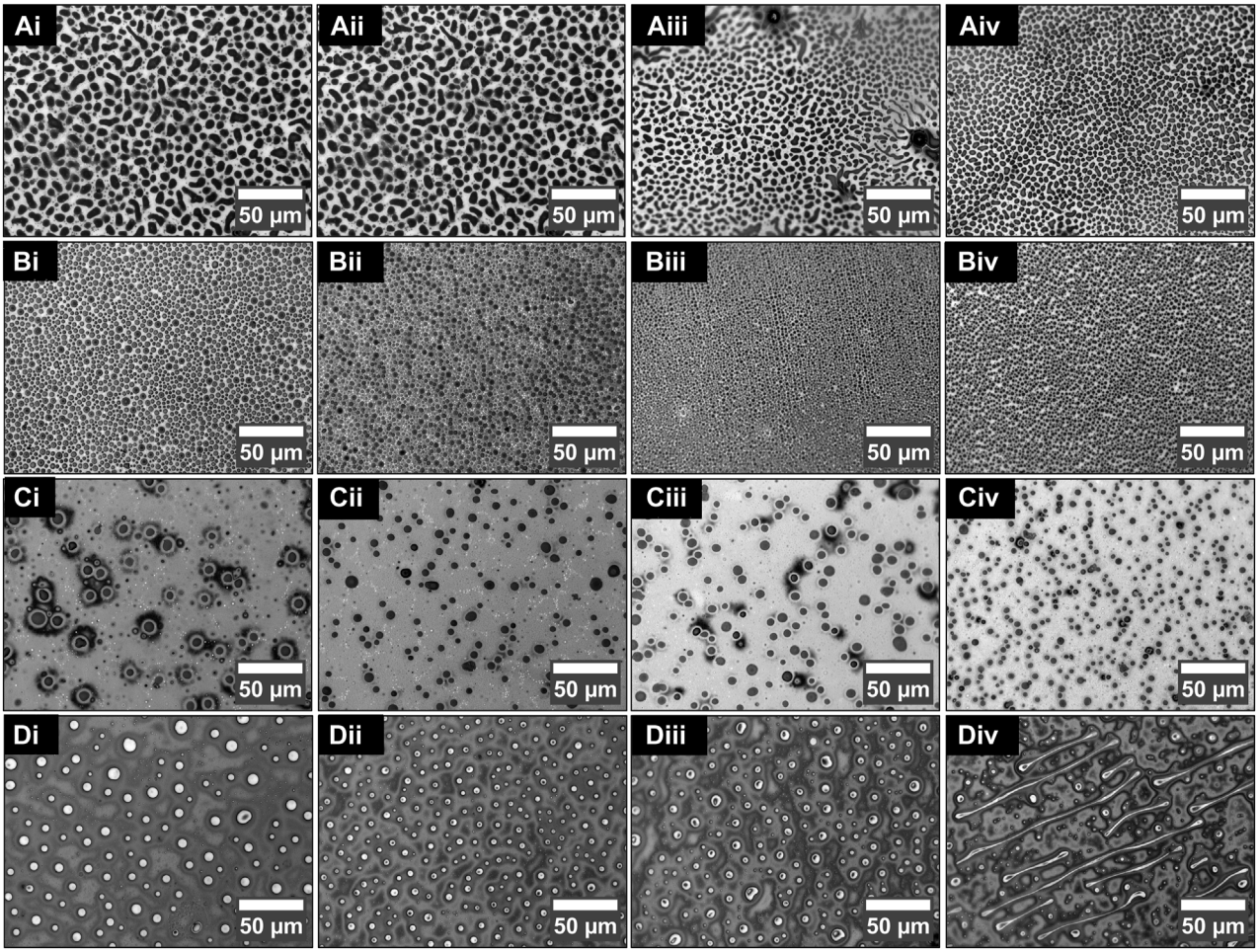

FIGURE 2
Morphology of the blended film with different concentrations and spin coated at different speeds. **(A)** 1:1, **(B)** 2:1, **(C)** 5:1, and **(D)** 1:5 (PS/PDMS) films deposited at **(i)** 1000 rpm, **(ii)** 3000 rpm, **(iii)** 5000 rpm, and **(iv)** 8000 rpm, respectively.

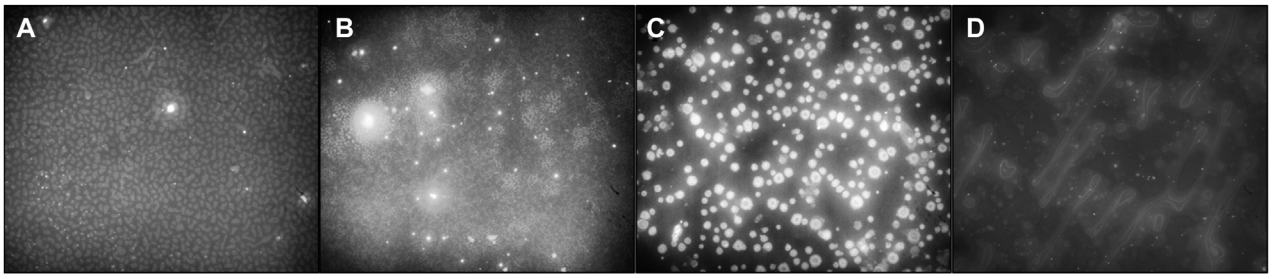

FIGURE 3
Fluorescent micrographs of the blended films. **(A)** 1:1, **(B)** 2:1, **(C)** 5:1, and **(D)** 1:5 (PS/PDMS) films at 8000 rpm.

and 1:5, respectively. The direction of the arrow in the picture represents the line on which the mapping was obtained. Upon comparing Figure 3A and Figure 2A (iv), it is evident that in the 1:1 film, the discontinuous hole-like structures are illuminated. This implies that the underlying polymer in Fig, 2a is that of PDMS, while the top layer of PS undergoes dewetting. This is also confirmed by the elemental mapping data shown in Figure 4A, according to which the carbon percentage increases slightly when moving from the exposed dewetted regions to the elevated regions of the films. Like 1:1, in both the 2:1 and 5:1 films (Figures 3B,C), the discontinuous dewetted circular regions show fluorescence and, hence, confirm the presence of an underlying PDMS layer, while the continuous PS

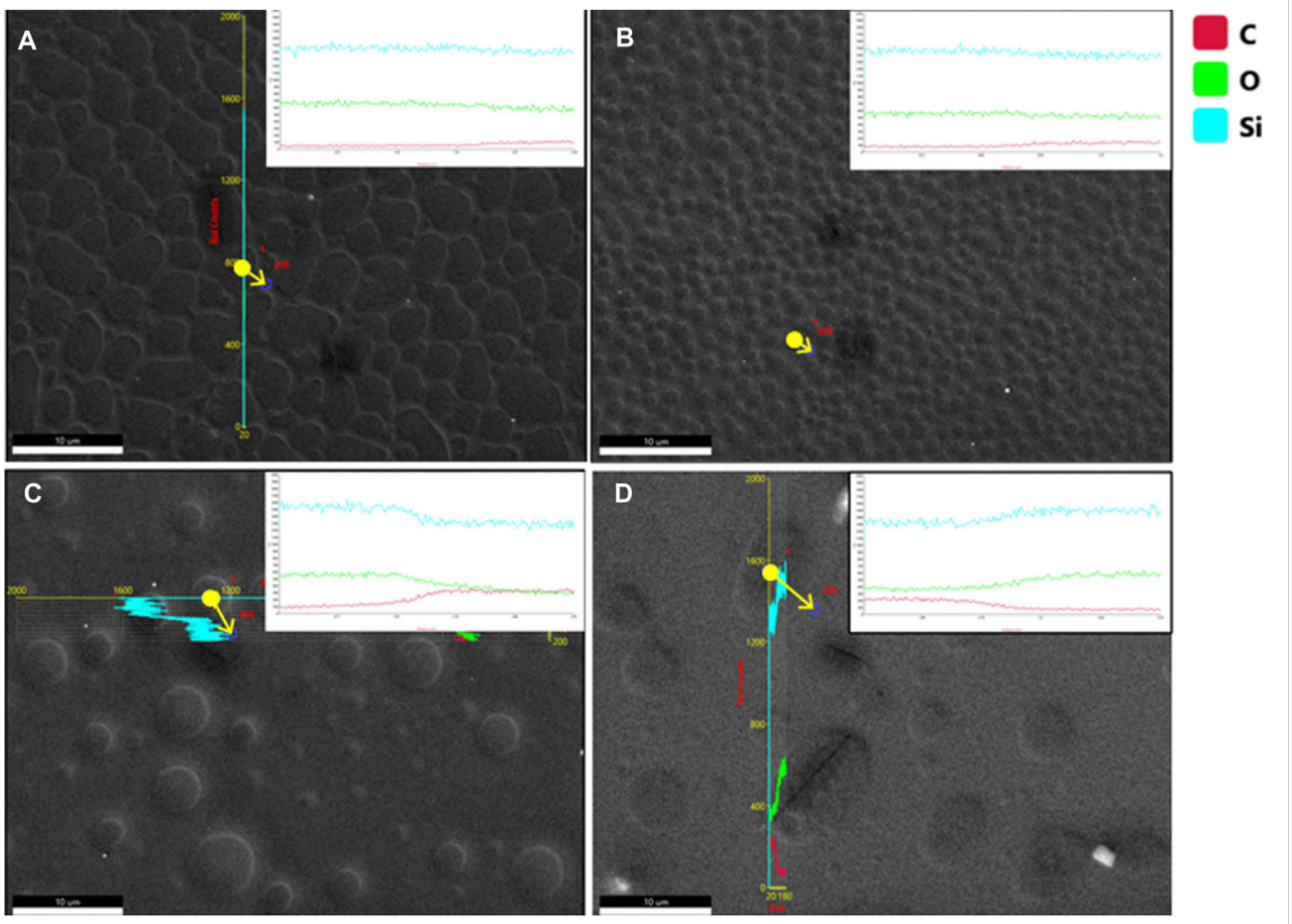

FIGURE 4
Elemental mapping showing the line EDX of the blended film at 8000 rpm. **(A)** 1:1, **(B)** 2:1, **(C)** 5:1, and **(D)** 1:5 (PS/PDMS) films.

layer at the top remains dark. The illuminated holes are, however, seen to be lesser in number in the 5:1 films (Figure 3C) compared to the 2:1 films (Figure 3B), as expected. Figures 4B,C, respectively, show the elemental mapping of the 2:1 and 5:1 films. In both of these, we can observe a decrease in the elemental levels of silicon and oxygen and an increase in the elemental level of carbon. The carbon content in one unit of PS is higher than in one unit of PDMS, while silicon is only present in PDMS and not in PS. Since the number of dewetted holes is significantly less in 5:1 films than in 2:1 films, the decrease in silicon and oxygen is considerably higher in 5:1 films when compared to 2:1 films due to the suppression of dewetting because of the higher PS concentration. In the 1:5 films (Figure 3D), it is evident that the fluorescent dye has penetrated the PDMS tubules, resulting in their illumination, while the now-underlying PS film remains dark. The elemental mapping of the 1:5 (PS/PDMS) films (Figure 4D) shows an increase in levels of elemental silicon and oxygen when moving toward the background, while the level of carbon decreases. This is likely due to the dewetting of the thin layer of PS in the background, which leads to the picking up of an elemental signal from the glass slide, which makes up the substrate for thin film deposition.

Temperature also plays an important role in controlling the morphology of the polymer films. Figure 5A (i–iv) shows the PS/PDMS thin films spin coated at room temperature, while Figure 5B (i–iv) displays the films deposited at 70°C. The 1:1 films prepared at room temperature show discrete, discontinuous, isolated hole-like structures exposing underlying PDMS, while the thin blended films prepared at 70°C show a continuous exposed structure of underlying PDMS. There is a phase inversion that occurs. The continuous structure of the top PS at room temperature now starts to disintegrate due to the coalescence of the holes. When the concentration of polystyrene increases in the solution to 2% and 5%, the hole size of the dewetted structures formed at room temperature and 70°C, respectively, increases from 3.37 µm (Figure 5Aii) to 4.75 µm (Figure 5Bii) for 2:1 blended films and from 4.87 µm (Figure 5A (iii)) to 6.95 µm (Figure 5B (iii)) for 5:1 blended films. If closely observed, it can be seen that the holes formed at a higher temperature for the 5:1 polymer blend (PS:PDMS) (Figure 5A (iv)) now show more angular/polygonal structures than perfectly circular structures, as in Figure 5A (iii). When the concentration of PS:PDMS is 1:5, as the temperature is increased from room temperature to 70°C, the average size of the PDMS structures decreases from 5.96 µm (Figure 5A (iv)) to 2.32 µm (Figure 5B (iv)), likely due to a decrease in the number density of tubes, which is now seen to break up into smaller spheres.

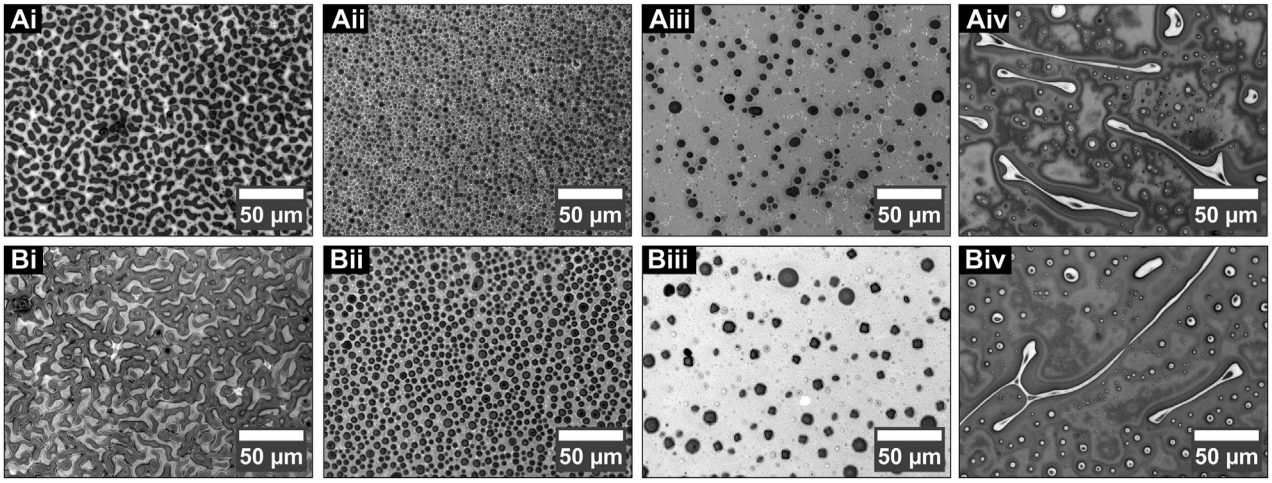

FIGURE 5
Morphology of the blended film at 8000 rpm with different concentrations and spin coated at different temperatures. **(i)** 1:1, **(ii)** 2:1, **(iii)** 5:1, and **(iv)** 1:5 (PS/PDMS) films deposited at **(A)** room temperature and **(B)** 70°C, respectively.

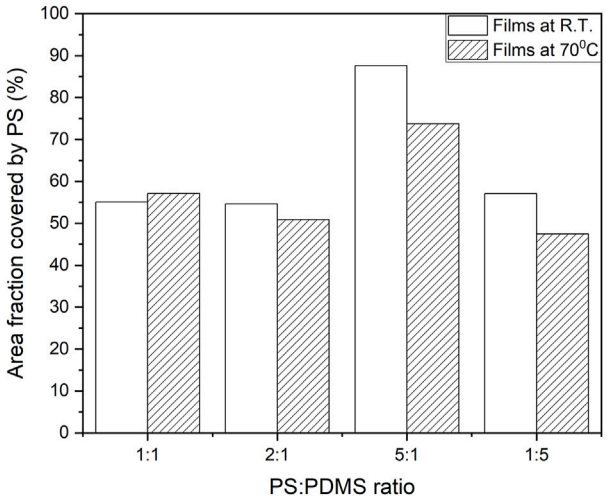

FIGURE 6
Graph showing the area fraction of the thin films covered by polystyrene at 8000 rpm for different PS/PDMS ratios.

A comparison of the area fraction of the films covered by PS with respect to the PS/PDMS ratio is shown in Figure 6. Because of the increased number density of holes, the fractional area coverage of the PS polymer is low for 1:1 (PS/PDMS) and 2:1 (PS/PDMS) films. As with higher concentrations, dewetting gets arrested, and the fractional area for PS is high for the 5:1 (PS/PDMS) films. With an increase in temperature, since dewetting kinetics increases, the PS fractional area either remains similar to corresponding morphologies at room temperature or, as expected, decreases in these films (refer to concentrations 1:1, 2:2, and 5:1 in Figure 6). For 1:5 polymer blends, since PDMS forms tubules and PS goes to the background, the surface area coverage for PS decreases. It decreases further for such films at higher temperatures since higher temperatures engender PDMS tubule breakage into smaller spheres.

AFM images of the blended films prepared at room temperature at 8000 rpm are shown in Figure 7, where Figures 7A–D correspond to the 1:1, 2:1, 5:1, and 1:5 blended films, respectively. The topographic images, as expected, reveal a non-uniform film with craters and columns throughout the film spread in a discrete manner. The craters in the film in Figures 7A–C result from PDMS exposure due to PS dewetting. The elevated rims and columns in these figures are those of PS. In Figure 7D, where the PDMS polymer concentration is high, the columns are formed due to the aggregation of PDMS in the film. The height of these features ranges from 100 to 500 nm. The peak height of the 1:1 films is shown to be 160 nm with a mean roughness of 21.79 nm, while the 2:1 films show a peak height of 350 nm and a mean roughness of 41.89 nm, the 5:1 films show a peak height of 117 nm and a surface roughness of 6.16 nm, and the 1:5 films show a peak height of 550 nm and a mean roughness of 101.5 nm. In the next section, we will try to uncover the physical reason behind the structure formation and the roughness achieved.

4 Discussion

The Flory–Huggins interaction parameter, or the polymer–solvent interaction parameter (also known as the $\chi_{P\text{-}S}$ parameter), is related to Hildebrand solubility parameters (δ; the square root of the cohesive energy density, i.e., the energy of vaporization per unit volume) of the polymer (P) and solvent (S):

$$\chi_{P-S} = \frac{V_s}{RT}(\delta_S - \delta_P)^2 + 0.34, \quad (1)$$

where V_S is the molar volume of the solvents, R is the universal gas constant, T is the temperature, and δ_S and δ_P are the solubility parameters of the solvent and polymer, respectively (Gong et al., 2006; Emerson et al., 2013). The lower value of χ implies higher interaction and mobility of the polymer chains. In our system, δ values for PS, PDMS, and toluene are 18.6, 15.0, and 18.2 $MPa^{1/2}$,

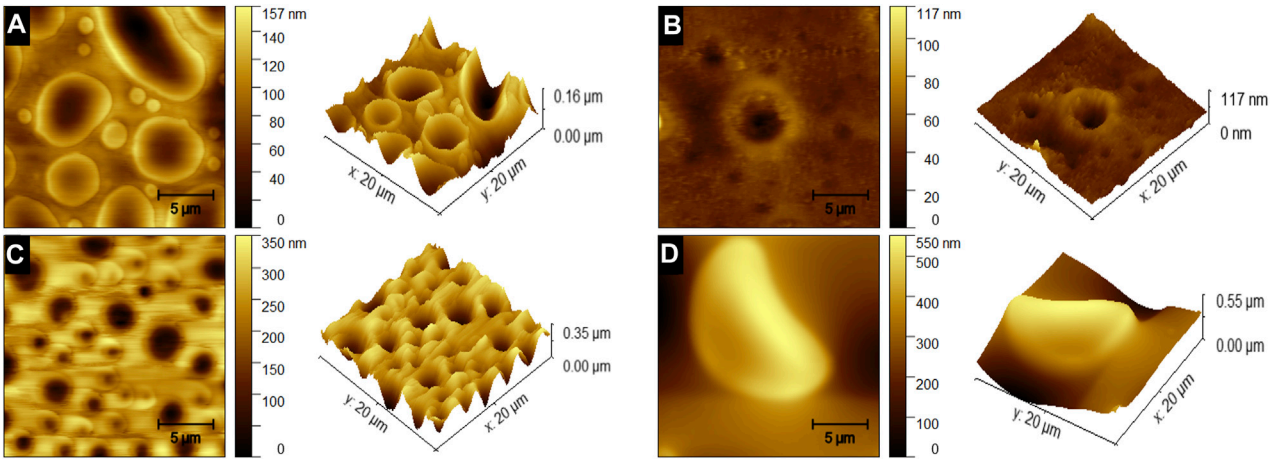

FIGURE 7
AFM images of the blended PS/PDMS films at 8000 rpm for **(A)** 1:1, **(B)** 2:1, **(C)** 5:1, and **(D)** 1:5 (PS/PDMS) films, respectively.

respectively (Gong et al., 2006; T; Wang et al., 2014). The solubility parameter of polystyrene in toluene is, thus, 0.347, and for PDMS in toluene, it is 0.779, according to Eq. 1. Thus, based on the values of χ, PS has a higher interaction and mobility in toluene compared to PDMS (Roy and Sharma, 2015).

Because of the immiscible nature of the polymer blend, as the solvent evaporates, the two polymers rapidly phase-separate and form a bilayer. Since PDMS has a higher density and lower mobility, it forms the bottom layer and PS forms a thin top layer (for PS: PDMS ratios 1:1, 2:2, and 5:1). However, the adhesive interaction between PS and PDMS leads to dewetting of the PS layer from the underlying polymer, which acts like a substrate. The dewetting leads to the uncovering of the substrate in the dewetted patches. As PS concentration increases in films with PS:PDMS ratios of 1:1, 2:1, and 5:1, the thickness of the film increases. For spinodal dewetting of a thin film over a substrate, the length scales (λ) of the dewetted holes is found to scale as h_0^2, where h_0 is the mean thickness of the film (Kotni et al., 2014; 2017). Thus, as the thicknesses of the films increase in 5:1 films (refer to Figure 2C; Figures 3C; Figure 5Aiii; Figures 7C; and Supplementary Figure S1C) compared to 2:1 films (refer to Figure 2B; Figures 3B; Figure 5Aii, Figures 7B; and Supplementary Figure S1B), the number density of holes is found to be lesser and situated at greater distances. Since the surface tension forces for films with larger thicknesses are higher (Sarkar and Sharma, 2010), one can also see more circular hole formation in 5:1 films compared to 2:1 films (refer to the optical images of Figure 2C and SEM images of Supplementary Figure S1C).

The smaller the thickness of the dewetting film (PS), the faster the film rupture process and dewetting kinetics (where the time of rupture $t_r \propto h_0^5$ (Kotni et al., 2014; 2017). As a result, at the same reference time, one can see that while a 2:1 (PS:PDMS) polymer blend (Figure 2B) shows several depressions (black and gray), 1:1 (PS:PDMS) polymer blend (Figure 2A) films with smaller thicknesses reveal mostly dark polygonal dewetted patches. For higher-thickness 2:1 polymer blend, some of the depressions are relatively at higher elevations (hence gray in color) and yet to reach the underlying PDMS surface; on the other hand, others reach the polymer–polymer interface and rupture, uncovering the underlying PDMS surface, leading to dewetting and the appearance of "black holes." Different elevations of the depressions/holes are also evident from the AFM images in Figure 7B, where the shades of brown illustrate different local thicknesses in the film. The different sizes of the holes are also apparent. While the depressions at higher elevations have smaller diameters, the dewetted holes (dark-brown-colored holes in Figure 7B) at the PDMS substrate start growing and, hence, show bigger diameters. For thinner films with 1: 1 blend, the kinetics is faster, as evident from the fact that at the same reference time, the higher elevated depressions are almost missing in these films, and most of the depressions can be seen to have reached the bottom PDMS layer, causing rupture and the formation of dark dewetted patches (refer to Figure 2A; Figure 7A). A comparison of the corresponding morphologies of Figures 2A,B reveals that the size of the growing dewetted holes in Figure 2A is larger than that of the deepening and growing holes in Figure 2B at a particular instance of time. A change in thickness can also be brought about by a change in rotational speed. In subsequent rows of Figures 2A–D, as one moves from figures i-iv as the rotational speed increases, the centrifugal force also increases, which engenders better spreading, leading to a decrease in film thickness for films having the same concentration ratio. Since, with lower film thickness, the patterns formed are at lower length scales, the number density of patterns increases as one moves from left to right in each of the rows of Figures 2A–D.

When the concentration of PDMS is higher than that of PS, the PDMS–PS blend again phase separates when spin coated. Since the cohesive force in PDMS increases with higher concentrations, PDMS polymer aggregates to give rise to spherical structures, while PS forms the underlying layer, as evident from the optical (Figure 2D; Figure 3D; Figure 5A,Biv), SEM (Supplementary Figure S1D), and AFM (Figure 7D) images. An increase in centrifugal force leads to increased shear during spin coating, which either is found to increase the number density of the spheres, similar to the increase in the number density of patterns formed in PS–PDMS blends with high PS concentrations (Figures 2A–C), or is found to cluster the spheres into elongated tubular structures (Figures 2D–2iv).

An increase in operating temperature normally decreases the viscosity and, thereby, increases the mobility of any polymer

(Roudat et al., 2004). Enhanced temperature has a similar influence on surface tension. An increase in temperature decreases the surface tension values. As a result, when the PS film interface interacts with the PDMS film interface to undergo dewetting, the mobility is faster; moreover, the restraining surface tension forces also decrease, and as a result, dewetting kinetics fasten. The dewetted patterns now become more coarsened (compare the morphologies in Figure 5A to the corresponding topologies in Figure 5B). The lowered surface tension effects are also visible from the more angular dewetted holes formed at elevated temperatures (refer to Figure 5B (iii)). For blends with a 1:5 PS:PDMS ratio, the faster kinetics at higher temperatures assist in breaking down the tubular structure.

Fabrication of miniaturized patterns with high surface roughness is ideal for enhancing functional properties. In 1:1 polymer blends, though the mean thicknesses are less, which leads to reduced length scales, because of faster kinetics, the morphologies become coarsened, leading to lowered roughness, whereas for 5:1 films, because of the larger mean thickness, the dewetting is suppressed, which again leads to less-rough films. From the study, it can be seen that 2:1 PS:PDMS blends at 8000 rpm were found to be ideally rough, with a peak height of 350 nm and a mean roughness of 41.89 nm for films having a higher PS concentration than PDMS concentration. However, for films with higher PDMS concentrations, the increased coalescence effect leads to elongated and rough protruding structures with a peak height of 550 nm and a mean roughness of 101.5 nm at 8000 rpm and room temperature. So, if porous structures with high roughness are required, moderately higher PS:PDMS ratios are preferred, whereas if protruded hydrophobic structures are required, one should go for fractional values of PS:PDMS concentrations.

Conclusion

Thin films fabricated by blending two dissimilar polymers in a common solvent and spin coating provide an easy method of obtaining self-organized, patterned surfaces without the need for expensive and complicated lithographic processes. The polystyrene–polydimethylsiloxane films produced by us show a bilayer structure with the formation of regular patterns, which can be controlled by varying the concentration of the polymers in the solution, spin-coating speed, and temperature at the time of fabrication of the films. The bilayer nature of the film is a result of the phase separation between the two polymers, which gives rise to spherical droplets, holes, bi-continuous lamellar structures, and tubular structures in the film. For PS:PDMS ratios less than 1 and for moderately valued films with ratios greater than 1, higher rotational speeds and lower temperatures are all favorable conditions to produce patterns with high surface roughness. This makes the thin blended films very versatile in nature, as they can be used in various applications involving catalysis, in the fabrication of antibiofouling membranes, coatings on biomedical implants, the creation of functionalized surfaces, etc. These blended films have the potential to be functionalized further for specialized applications by subjecting them to surface modifications and the addition of nanoparticles.

Data availability statement

The raw data supporting the conclusion of this article will be made available by the authors, without undue reservation.

Author contributions

SA: formal analysis, investigation, methodology, validation, visualization, writing–original draft, and writing–review and editing. ML: data curation, formal analysis, investigation, project administration, resources, supervision, and writing–review and editing. JS: conceptualization, formal analysis, funding acquisition, investigation, methodology, project administration, resources, supervision, visualization, writing–original draft, and writing–review and editing.

Funding

The author(s) declare financial support was received for the research, authorship, and/or publication of this article. SA sincerely acknowledges the Council for Scientific and Industrial Research (CSIR) for NET-JRF Fellowship and UQ-IITD Academy of Research (UQIDAR) for providing administrative and financial support.

Conflict of interest

The authors declare that the research was conducted in the absence of any commercial or financial relationships that could be construed as a potential conflict of interest.

Publisher's note

Supplementary material

The Supplementary Material for this article can be found online at: https://www.frontiersin.org/articles/10.3389/frsfm.2023.1306346/full#supplementary-material

References

Arias, A. C., Corcoran, N., Banach, M., Friend, R. H., MacKenzie, J. D., and Huck, W. T. S. (2002). Vertically segregated polymer-blend photovoltaic thin-film structures through surface-mediated solution processing. *Appl. Phys. Lett.* 80 (10), 1695–1697. doi:10.1063/1.1456550

Arias-Zapata, J., Böhme, S., Garnier, J., Girardot, C., Antoine, L., and Zelsmann, M. (2016). Ultrafast assembly of PS-PDMS block copolymers on 300 mm wafers by blending with plasticizers. *Adv. Funct. Mater.* 26 (31), 5690–5700. doi:10.1002/adfm.201601469

Basu, S., Bhukya, V. N., Ankarao, K., Patra, P., and Sarkar, J. (2021). Self-assembly of graphene nano-particles on biocompatible polymer through dewetting. *Surfaces Interfaces* 23 (2021), 101009. doi:10.1016/j.surfin.2021.101009

Basu, S., and Sarkar, J. (2019). Selective adsorption of oil on self-organized surface patterns formed over soft thin PDMS films. *Chem. Eng. Sci.* 207, 970–979. doi:10.1016/j.ces.2019.07.021

Bhandaru, N. (2020). Solvo-selective imprinting of a thin polymer blend film for creating multi-length scale patterns. *Bull. Mater. Sci.* 43 (1), 180. doi:10.1007/s12034-020-02156-w

Björström, C. M., Nilsson, S., Bernasik, A., Budkowski, A., Andersson, M., Magnusson, K. O., et al. (2007). Vertical phase separation in spin-coated films of a low bandgap polyfluorene/PCBM blend—effects of specific substrate interaction. *Appl. Surf. Sci.* 253 (8), 3906–3912. doi:10.1016/j.apsusc.2006.08.024

Böltau, M., Walheim, S., Mlynek, J., Krausch, G., and Steiner, U. (1998). Surface-induced structure formation of polymer blends on patterned substrates. *Nature* 391 (6670), 877–879. doi:10.1038/36075

Budkowski, A. (1999). Interfacial phenomena in thin polymer films: phase coexistence and segregation. *Interfaces Cryst. Viscoelasticity*, 1–111. doi:10.1007/3-540-48836-7_1

Budkowski, A., Bernasik, A., Cyganik, P., Raczkowska, J., Penc, B., Bergues, K., et al. (2003). Substrate-determined shape of free surface profiles in spin-cast polymer blend films. *Macromolecules* 36 (11), 4060–4067. doi:10.1021/ma0208943

Cai, H., Zheng, B., Zhu, D., Wu, Y., Cardinaels, R., Moldenaers, P., et al. (2023). Regulation of dewetting and morphology evolution in spin-coated PS/PMMA blend films via graphene-based Janus nanosheets. *Appl. Surf. Sci.* 630 (2023), 157393. doi:10.1016/j.apsusc.2023.157393

Cui, L., Ding, Y., Xue, Li, Wang, Z., and Han, Y. (2006). Solvent and polymer concentration effects on the surface morphology evolution of immiscible polystyrene/poly (methyl methacrylate) blends. *Thin Solid Films* 515 (4), 2038–2048. doi:10.1016/j.tsf.2006.04.045

Das, A., Arka, B. D., Chattopadhyay, S., De, G., Sanyal, M. K., and Mukherjee, R. (2020). Nanoparticle induced morphology modulation in spin coated PS/PMMA blend thin films. *Langmuir* 36 (50), 15270–15282. doi:10.1021/acs.langmuir.0c02584

Dhara, P., and Mukherjee, R. (2021). Phase separation and dewetting of polymer dispersed liquid crystal (PDLC) thin films on flat and patterned substrates. *J. Mol. Liq.* 341 (2021), 117360. doi:10.1016/j.molliq.2021.117360

El-Mabrouk, K., Mohamed, B., and Bousmina, M. (2007). Phase separation in PS/PVME thin and thick films. *J. colloid interface Sci.* 306 (2), 354–367. doi:10.1016/j.jcis.2006.10.051

Emerson, J. A., Toolan, D. T. W., Howse, J. R., Furst, E. M., and Epps, T. H., III. (2013). Determination of solvent–polymer and polymer–polymer Flory–Huggins interaction parameters for poly (3-hexylthiophene) via solvent vapor swelling. *Macromolecules* 46 (16), 6533–6540. doi:10.1021/ma400597j

Escalé, P., Rubatat, L., Billon, L., and Save, M. (2012). Recent advances in honeycomb-structured porous polymer films prepared via breath figures. *Eur. Polym. J.* 48 (6), 1001–1025. doi:10.1016/j.eurpolymj.2012.03.001

Ferreiro, V., Douglas, J. F., Warren, J. A., and Karim, A. (2002). Nonequilibrium pattern formation in the crystallization of polymer blend films. *Phys. Rev. E* 65 (4), 042802. doi:10.1103/physreve.65.042802

Fu, Y. F., Yuan, C. Q., and Bai, X. Q. (2017). Marine drag reduction of shark skin inspired riblet surfaces. *Biosurface Biotribology* 3 (1), 11–24. doi:10.1016/j.bsbt.2017.02.001

Gong, Y., Huang, H., Hu, Z., Chen, Y., Chen, D., Wang, Z., et al. (2006). Inverted to normal phase transition in solution-cast Polystyrene– poly (methyl methacrylate) block copolymer thin films. *Macromolecules* 39 (9), 3369–3376. doi:10.1021/ma052380k

Guo, Y., and Ren, S. (2021). Bilayer PMMA antireflective coatings via microphase separation and MAPLE. *J. Polym. Eng.* 41 (2), 164–173. doi:10.1515/polyeng-2020-0198

Helberg, R. M. L., Dai, Z., Ansaloni, L., and Deng, L. (2020). PVA/PVP blend polymer matrix for hosting carriers in facilitated transport membranes: synergistic enhancement of CO2 separation performance. *Green Energy and Environ.* 5 (no. 1), 59–68. doi:10.1016/j.gee.2019.10.001

Hou, S., Yu, J., Zhuang, X., Li, D., Liu, Y., Gao, Z., et al. (2019). Phase separation of P3HT/PMMA blend film for forming semiconducting and dielectric layers in organic thin-film transistors for high-sensitivity NO2 detection. *ACS Appl. Mater. interfaces* 11 (47), 44521–44527. doi:10.1021/acsami.9b15651

Jager, E. W. H., Smela, E., and Inganas, O. (2000). Microfabricating conjugated polymer actuators. *Science* 290 (5496), 1540–1545. doi:10.1126/science.290.5496.1540

Kargupta, K., and Sharma, A. (2001). Templating of thin films induced by dewetting on patterned surfaces. *Phys. Rev. Lett.* 86, 4536–4539. doi:10.1103/physrevlett.86.4536

Kästner, C., Rathgeber, S., Egbe, D. A. M., and Hoppe, H. (2013). Improvement of photovoltaic performance by ternary blending of amorphous and semi-crystalline polymer analogues with PCBM. *J. Mater. Chem. A* 1 (12), 3961–3969. doi:10.1039/c3ta01070h

Köse, M. E., Crutchley, R. J., DeRosa, M. C., Ananthakrishnan, N., Reynolds, J. R., and Schanze, K. S. (2005). Morphology and oxygen sensor response of luminescent Ir-labeled poly (dimethylsiloxane)/polystyrene polymer blend films. *Langmuir* 21 (18), 8255–8262. doi:10.1021/la051146k

Kotni, T. R., Khanna, R., and Sarkar, J. (2017). Kinetics of sub-spinodal dewetting of thin films of thickness dependent viscosity. *J. Phys. Condens. Matter* 29 (17), 175001. doi:10.1088/1361-648x/aa62d9

Kotni, T. R., Sarkar, J., and Khanna, R. (2014). Kinetically engendered subspinodal length scales in spontaneous dewetting of thin liquid films. *Phys. Rev. E* 90 (2), 020401. doi:10.1103/physreve.90.020401

Kumar, R., Rahman, H., Ranwa, S., Kumar, A., and Kumar, G. (2020). Development of cost effective metal oxide semiconductor based gas sensor over flexible chitosan/PVP blended polymeric substrate. *Carbohydr. Polym.* 239, 116213. doi:10.1016/j.carbpol.2020.116213

Latthe, S. S., Terashima, C., Nakata, K., and Fujishima, A. (2014). Superhydrophobic surfaces developed by mimicking hierarchical surface morphology of lotus leaf. *Molecules* 19 (4), 4256–4283. doi:10.3390/molecules19044256

Li, X., Han, Y., and An, L. (2003). Surface morphology control of immiscible polymer-blend thin films. *Polymer* 44 (26), 8155–8165. doi:10.1016/j.polymer.2003.10.012

Luo, R., Li, H., Du, B., Zhou, S., and Zhu, Y. (2020). A simple strategy for high stretchable, flexible and conductive polymer films based on PEDOT: PSS-PDMS blends. *Org. Electron.* 76, 105451. doi:10.1016/j.orgel.2019.105451

Luo, T., Zheng, L., Chen, D., Zhang, C., Liu, S., Jiang, C., et al. (2023). Implantable microfluidics: methods and applications. *Analyst* 148, 4637–4654. doi:10.1039/d3an00981e

McDougal, A., Miller, B., Singh, M., and Kolle, M. (2019). Biological growth and synthetic fabrication of structurally colored materials. *J. Opt.* 21 (7), 073001. doi:10.1088/2040-8986/aaff39

Mo, Y., Xue, P., Yang, Q., Liu, H., Zhao, Xu, Wang, J., et al. (2021). Composite slow-release fouling release coating inspired by synergistic anti-fouling effect of scaly fish. *Polymers* 13 (16), 2602. doi:10.3390/polym13162602

Mrđenović, D., Abbott, D., Mougel, V., Su, W., Kumar, N., and Zenobi, R. (2022). Visualizing surface phase separation in PS-PMMA polymer blends at the nanoscale. *ACS Appl. Mater. Interfaces* 14 (21), 24938–24945. doi:10.1021/acsami.2c03857

Müller-Buschbaum, P. (2003). Dewetting and pattern formation in thin polymer films as investigated in real and reciprocal space. *J. Phys. Condens. Matter* 15 (36), R1549–R1582. doi:10.1088/0953-8984/15/36/201

Müller-Buschbaum, P., Bauer, E., Wunnicke, O., and Stamm, M. (2005). The control of thin film morphology by the interplay of dewetting, phase separation and microphase separation. *J. Phys. Condens. Matter* 17 (9), S363–S386. doi:10.1088/0953-8984/17/9/006

Okerberg, B. C., Marand, H., and Douglas., J. F. (2008). Dendritic crystallization in thin films of PEO/PMMA blends: a comparison to crystallization in small molecule liquids. *Polymer* 49 (2), 579–587. doi:10.1016/j.polymer.2007.11.034

Raczkowska, J., Bernasik, A., Budkowski, A., Sajewicz, K., Penc, B., Lekki, J., et al. (2004). Structures formed in spin-cast films of polystyrene blends with poly (butyl methacrylate) isomers. *Macromolecules* 37 (19), 7308–7315. doi:10.1021/ma035815h

Roudaut, G., Simatos, D., Champion, D., Contreras-Lopez, E., and Le Meste, M. J. I. F. S. (2004). Molecular mobility around the glass transition temperature: a mini review. *Innovative Food Sci. Emerg. Technol.* 5 (2), 127–134. doi:10.1016/j.ifset.2003.12.003

Roy, S., and Sharma, A. (2015). Self-organized morphological evolution and dewetting in solvent vapor annealing of spin coated polymer blend nanostructures. *J. colloid interface Sci.* 449, 215–225. doi:10.1016/j.jcis.2014.12.095

Saleem, J., Moghal, Z. K. B., Usman, B. S., Luque, R., and McKay, G. (2023). Mixed plastics waste valorization to high-added value products via thermally induced phase separation and spin-casting. *Green Energy and Environ.*, doi:10.1016/j.gee.2023.08.004

Sarkar, J., and Sharma, A. (2010). A unified theory of instabilities in viscoelastic thin films: from wetting to confined films, from viscous to elastic films, and from short to long waves. *Langmuir* 26 (11), 8464–8473. doi:10.1021/la9049007

Sharma, A., and Reiter, G. (1996). Instability of thin polymer films on coated substrates: rupture, dewetting, and drop formation. *J. Colloid Interface Sci.* 178 (2), 383–399. doi:10.1006/jcis.1996.0133

Sirringhaus, H., Tessler, N., and Friend, R. H. (1998). Integrated optoelectronic devices based on conjugated polymers. *Science* 280 (5370), 1741–1744. doi:10.1126/science.280.5370.1741

Sohn, E.-Ho, Kim, B. G., Chung, J.-S., Kang, H., and Lee, J.-C. (2011). Wettability of the morphologically and compositionally varied surfaces prepared from blends of well ordered comb-like polymer and polystyrene. *J. colloid interface Sci.* 354 (2), 650–661. doi:10.1016/j.jcis.2010.10.068

Tanaka, K., Takahara, A., and Kajiyama, T. (1996). Film thickness dependence of the surface structure of immiscible polystyrene/poly (methyl methacrylate) blends. *Macromolecules* 29 (9), 3232–3239. doi:10.1021/ma951140+

Ton-That, C., Shard, A. G., and Bradley, R. H. (2002). Surface feature size of spin cast PS/PMMA blends. *Polymer* 43 (18), 4973–4977. doi:10.1016/s0032-3861(02)00333-6

Ton-That, C., Shard, A. G., Daley, R., and Bradley, R. H. (2000). Effects of annealing on the surface composition and morphology of PS/PMMA blend. *Macromolecules* 33 (22), 8453–8459. doi:10.1021/ma000792h

Tu, T. T. K., Han, J. W., Dong, W., Yeun, T. J., Yeong, S. G., Bach, L. G., et al. (2019a). Enhancement of light extraction from Organic Light-Emitting Diodes by SiO2 nanoparticle-embedded phase separated PAA/PI polymer blends. *Mol. Cryst. Liq. Cryst.* 686 (1), 55–62. doi:10.1080/15421406.2019.1648036

Tu, T. T. K., Joo, W., Kim, D. W., Kim, Y. H., Ahn, B.-H., and Kwon, T. (2019b). Formation of nanopore and nanopillar patterned polymer films from mixed PAA-PI solutions by phase separation method. *Mol. Cryst. Liq. Cryst.* 679 (1), 80–86. doi:10.1080/15421406.2019.1597549

Virumbrales-Muñoz, M., Livingston, M. K., Farooqui, M., Skala, M. C., Beebe, D. J., and Ayuso, J. M. (2019). Development of a microfluidic array to study drug response in breast cancer. *Molecules* 24 (23), 4385. doi:10.3390/molecules24234385

Walheim, S., Böltau, M., Mlynek, J., Krausch, G., and Steiner, U. (1997). Structure formation via polymer demixing in spin-cast films. *Macromolecules* 30 (17), 4995–5003. doi:10.1021/ma9619288

Walheim, S., Ramstein, M., and Steiner, U. (1999). Morphologies in ternary polymer blends after spin-coating. *Langmuir* 15 (14), 4828–4836. doi:10.1021/la981467e

Wang, M., Braun, H.-G., and Meyer, E. (2003). Crystalline structures in ultrathin poly (ethylene oxide)/poly (methyl methacrylate) blend films. *Polymer* 44 (17), 5015–5021. doi:10.1016/s0032-3861(03)00492-0

Wang, M., Braun, H.-G., and Meyer, E. (2004). Transition of crystal growth as a result of changing polymer states in ultrathin poly (ethylene oxide)/poly (methyl methacrylate) blend films with thickness of< 3 nm. *Macromolecules* 37 (2), 437–445. doi:10.1021/ma0355812

Wang, T., Zhang, C., Zhao, R., Zhu, C., Yang, C., and Liu, C. (2014). Solvent extraction of bitumen from oil sands. *Energy and fuels* 28 (4), 2297–2304. doi:10.1021/ef402101s

Wei, M., Fang, L., Lee, J., Somu, S., Xiong, X., Barry, C., et al. (2009). Directed assembly of polymer blends using nanopatterned templates. *Adv. Mater.* 21 (7), 794–798. doi:10.1002/adma.200802052

Xia, Y., Kim, E., Zhao, X.-M., Rogers, J. A., Prentiss, M., and Whitesides, G. M. (1996). Complex optical surfaces formed by replica molding against elastomeric masters. *Science* 273 (5273), 347–349. doi:10.1126/science.273.5273.347

Xue, L., and Han, Y. (2011). Pattern formation by dewetting of polymer thin film. *Prog. Polym. Sci.* 36 (2), 269–293. doi:10.1016/j.progpolymsci.2010.07.004

Xue, L., Zhang, J., and Han, Y. (2012). Phase separation induced ordered patterns in thin polymer blend films. *Prog. Polym. Sci.* 37 (4), 564–594. doi:10.1016/j.progpolymsci.2011.09.001

Ye, C., Singh, G., Wadley, M. L., Karim, A., Cavicchi, K. A., and Vogt, B. D. (2013). Anisotropic mechanical properties of aligned polystyrene-block-polydimethylsiloxane thin films. *Macromolecules* 46 (21), 8608–8615. doi:10.1021/ma401780r

Zhao, K., Ding, Z., Xue, L., and Han, Y. (2010). Crystallization-induced phase segregation based on double-crystalline blends of poly(3-hexylthiophene) and poly(ethylene glycol)s. *Macromol. rapid Commun.* 31 (6), 532–538. doi:10.1002/marc.200900770

Zuyderhoff, E. M., Dekeyser, C. M., Rouxhet, P. G., and Christine, C. (2008). An AFM, XPS and wettability study of the surface heterogeneity of PS/PMMA-r-PMAA demixed thin films. *J. colloid interface Sci.* 319 (1), 63–71. doi:10.1016/j.jcis.2007.11.007